Materials Letters 235 (2019) 224–227

Contents lists available at ScienceDirect

Materials Letters

journal homepage: www.elsevier.com/locate/mlblue

# Revealing the intrinsic ductility of electrodeposited nanocrystalline metals

Hiroki Mori [a], Isao Matsui [b,*], Yorinobu Takigawa [a], Tokuteru Uesugi [a], Kenji Higashi [a]

[a] Department of Materials Science, Osaka Prefecture University, 1-1, Gakuen-cho, Sakai, Osaka 599-8531, Japan
[b] Structural Materials Research Institute, National Institute of Advanced Industrial Science and Technology (AIST), 2266-98 Shimo-Shidami, Moriyama-ku, Nagoya 463-8560, Japan

ARTICLE INFO

*Article history:*
Received 3 August 2018
Received in revised form 4 October 2018
Accepted 7 October 2018
Available online 8 October 2018

*Keywords:*
Nanocrystalline metal deposition
Iron alloys
Ductility
Multiple regression analysis

ABSTRACT

We electrodeposited bulk nanocrystalline Fe–Ni alloys with a tensile ductility of 12%–24%. We explored the intrinsic ductility of these alloys, taking into consideration the relationship between the ductility and the orientation index and contents of the grain boundary embrittlement element. Applying multiple regression analysis to our findings and those from the literature we found that the ductility of Fe–Ni alloys can be predicted from their orientation index for the (2 0 0) plane and sulfur content. The analysis of our study points to the potential for intrinsic ductility in nanocrystalline Fe–Ni alloys greater than that of the present highest value of 24%.



## 1. Introduction

Mechanical behavior of nanocrystalline metals and alloys with grain sizes less than 100 nm has attracted considerable attention [1]. To reveal the mechanical properties, many techniques for producing nanocrystalline materials have been developed [1]. The development of these fabrication processes has realized high-strength alloys [2,3]. However, demonstrations of plasticity in nanocrystalline materials have been limited [2,3]. The conditions for producing grain sizes less than 100 nm often require the formation of nanocrystalline metals with defects, high internal stresses, and high levels of impurities. Recent studies [4,5] have indicated that overcoming these problems could allow bulk nanocrystalline metals and alloys to exhibit a high-tensile ductility of approximately 10% combined with high strength. Unfortunately, these efforts have not provided an answer to the question of whether a sample is exhibiting its highest potential ductility in the absence of harmful effects (intrinsic ductility). It is not clear how much further it might be possible to improve ductility in bulk nanocrystalline metals and alloys.

In our previous studies, we successfully developed a new electrodeposition system that could produce bulk nanocrystalline Fe–Ni alloys with a tensile ductility of 6%–16% [6,7]. However, it is not clear that the highest tensile ductility of 16% is an intrinsic limit of these alloys. Research on electrodeposited Ni–W alloys has indicated that free lateral growth, a growth mode during electrodeposition [8], results in artifact-free electrodeposits and (2 0 0)-orientated structures [9]. Under these conditions the tensile ductility considerably increases from 0% to 13% with a greater orientation index for (2 0 0) plane, $I_{200}$ [5]. The value of $I_{200}$ is an indicator of the abundance of defects and useful for producing highly ductile bulk nanocrystalline electrodeposits. However, variation is typically observed in plots of tensile ductility versus $I_{200}$ for electrodeposited bulk nanocrystalline Fe–Ni alloys [6,7]. Thus, predictions of ductility based only on $I_{200}$ are inadequate. In the present paper, we electrodeposited bulk nanocrystalline Fe–Ni alloys with strongly (2 0 0)-orientated structures, under various deposition conditions to determine the factors that affect tensile ductility. The tensile behaviors of these alloys are discussed to provide insight into the intrinsic ductility of electrodeposited nanocrystalline metals and alloys.

## 2. Experimental methods

Three types of bulk samples of nanocrystalline Fe–Ni alloys were electrodeposited. Two types of deposition bath (LN and LM) containing different types of chloride were prepared. The details of these baths are described in [10], and the amount of saccharin sodium was reduced from 5.0 to 1.0 g/L. We assigned the following labels to the samples, corresponding to bath types and bath temperature: LN50, LM50, and LM55. All samples were electrodeposited in a 5-L bath system and the details of the system have been presented in a previous report [5]. Electrodepositions were

* Corresponding author.
*E-mail address:* i-matsui@aist.go.jp (I. Matsui).

https://doi.org/10.1016/j.matlet.2018.10.053
0167-577X/

performed at a current density of 10 mA/cm$^2$, bath temperatures of 50.0 or 55.0 °C and at a pH 2.1 ± 0.1. The pH values of the solutions were maintained by adding drops of 1.0 mol/L sulfamic acid.

The nickel content of the electrodeposited Fe–Ni alloys was measured by scanning electron microscopy with energy-dispersive X-ray spectrometry analysis (SEM–EDS, Hitachi S-4800). The sulfur contents were quantified by infrared (IR) absorption. To determine the preferential orientation of the samples, we measured X-ray diffraction (XRD, Rigaku Ultima IV) spectra using Cu Kα radiation. The microstructure was observed by transmission electron microscopy (TEM, JEOL ARM-200FC), operated at 200 kV. Dog-bone specimens with a gauge length of 12.0 mm, width of 4.0 mm, and thickness of approximately 0.8 mm were machined for tensile tests by electrical discharge machining from the as-deposited plates. Tensile tests were performed at a strain rate of $1 \times 10^{-3}$ s$^{-1}$ at room temperature. The plastic elongation of the specimen after fracturing was measured from the change in the gauge length.

## 3. Results and discussion

The Ni content of samples LN50, LM50, and LM55 were 45, 44, and 43 at.%, respectively. Their sulfur contents were 0.087, 0.066,

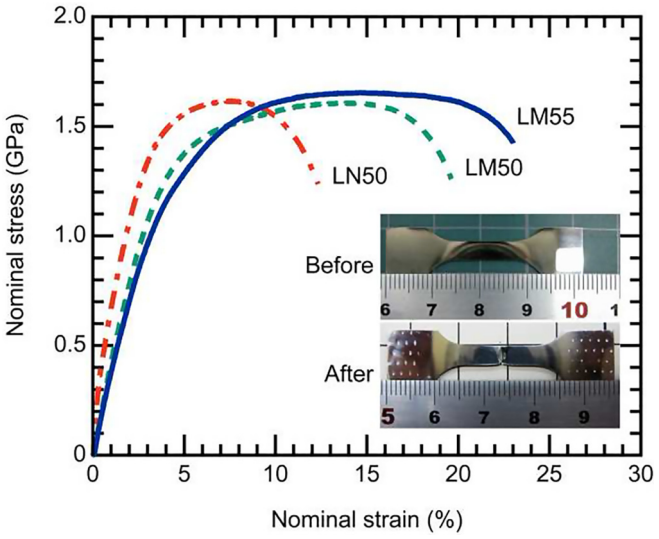


**Fig. 2.** Stress-strain curves of each sample. (inset) Photograph shows an actual LM55 tensile specimen with a high-tensile ductility of ~24%.

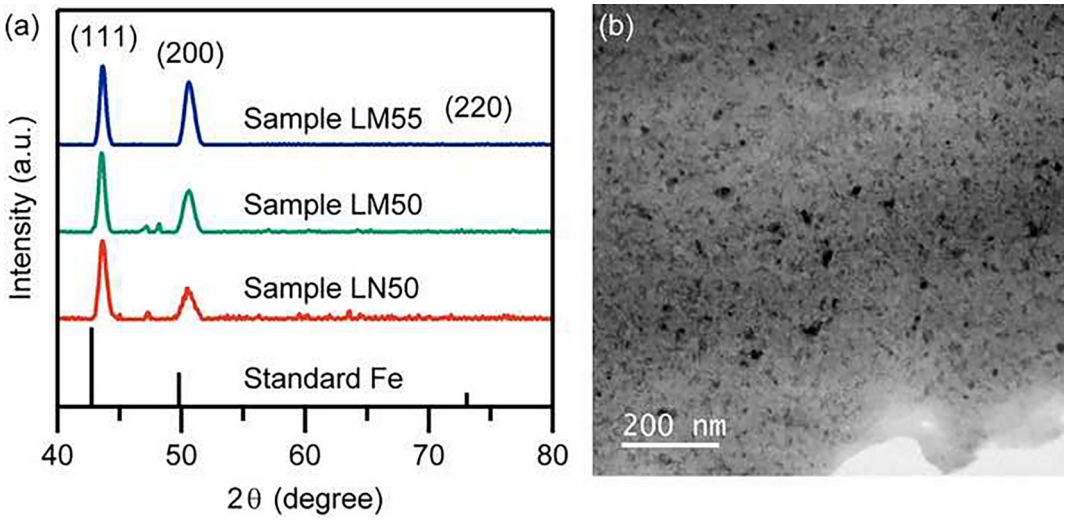


**Fig. 1.** (a) XRD pattern of each sample. (B) Bright-field STEM images of sample LM55.

**Table 1**
Experimental data for bulk nanocrystalline Fe–Ni alloys from the literature [6,7,10–13] and this study.

| Sample | S (at.%) | $I_{111}$ | $I_{200}$ | UTS (GPa) | $\varepsilon_f$ (%) |
|---|---|---|---|---|---|
| LN50 | 0.087 | 1.09 | 1.19 | 1.56 | 11.9 |
| LM50-1 | 0.066 | 1.04 | 1.27 | 1.60 | 19.3 |
| LM50-2 | 0.069 | 1.04 | 1.27 | 1.69 | 18.7 |
| LM55 | 0.069 | 0.89 | 1.64 | 1.65 | 23.8 |
| Fe-56Ni [6] | 0.098* | 1.36* | 0.72* | 1.87 | 5.5 |
| Fe-46Ni [6] | 0.085* | 1.33* | 0.47* | 1.68 | 6.4 |
| Fe-44Ni [6] | 0.071* | 1.23* | 0.78* | 1.65 | 15.8 |
| Fe-43Ni [6] | 0.082* | 1.28* | 0.66* | 1.61 | 11.8** |
| Fe-42Ni [13] | 0.071* | 1.30 | 0.70 | 1.56* | 13.2* |
| HM50-1 [10] | 0.062 | 1.29 | 0.67 | 1.64 | 17.8 |
| HM50-2 [10] | 0.063 | 1.26 | 0.75 | 1.63 | 19.1 |
| HN-1 [7] | 0.084 | 1.27 | 0.77 | 1.72 | 10.6 |
| HN-2 [7] | 0.089 | 1.20 | 0.92 | 1.77 | 10.1 |
| Fe-50Ni [11,12] | 0.107 | 0.97 | 1.43 | 1.72*** | 5.7*** |
| Fe-50Ni [11,12] | 0.107 | 0.97 | 1.43 | 1.71*** | 7.0*** |

* Our previous data which are not shown in Ref. [6].
** In Ref. [6], the highest value of 12.2% is shown but an average value of 11.8% was used in this paper.
*** These are the values converted from the true stress and true strain.